Study of zeolite clinoptilolite D-glucose adsorption properties in vitro and in vivo

Markoska, Rumenka; Stojković, Ranko; Filipović, Marko; Jurin, Mladenka; Špada, Vedrana; Kavre Pitaver, Ivna; Pavelić, Krešimir; MArković, Dean; Kraljević Pavelić, Sandra

Chemico-Biological Interactions 382 (2023) 110641

Contents lists available at ScienceDirect

Chemico-Biological Interactions

journal homepage: www.elsevier.com/locate/chembioint

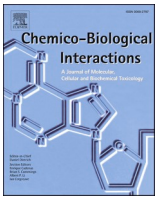

Research paper

Study of zeolite clinoptilolite D-glucose adsorption properties *in vitro* and *in vivo*

Rumenka Markoska [a,1], Ranko Stojković [b,1], Marko Filipović [d], Mladenka Jurin [c], Vedrana Špada [e], Ivna Kavre Piltaver [f], Krešimir Pavelić [d], Dean Marković [a], Sandra Kraljević Pavelić [g,*]

[a] University of Rijeka, Department of Biotechnology, Radmile Matejčić 2, 51000 Rijeka, Croatia
[b] Rudjer Boskovic Institute, Division of Molecular Medicine, Laboratory for Chiral Technologies, Bijenička cesta 54, 10000 Zagreb, Croatia
[c] Rudjer Boskovic Institute, Division of Organic Chemistry and Biochemistry, Laboratory for Chiral Technologies, Bijenička cesta 54, 10000 Zagreb, Croatia
[d] Juraj Dobrila University of Pula, Zagrebacka 30, 52100 Pula, Croatia
[e] Istarsko Veleučilište – Università Istriana di scienze applicate, Riva 6, 52100 Pula, Croatia
[f] University of Rijeka, Faculty of Physics and Centre for Micro- and Nanosciences and Technologies, Radmile Matejčić 2, 51000 Rijeka, Croatia
[g] University of Rijeka, Faculty of Health Studies, Ulica Viktora Cara Emina 5, 51 000 Rijeka, Croatia

ARTICLE INFO

Keywords:
Clinoptilolite
PMA-Zeolite
D-glucose
Mice
Sugar blood level

ABSTRACT

Beneficial effects of a natural zeolite clinoptilolite *in vivo* on mammals, including humans, have been empirically observed and documented in literature. The positive biological activities have been associated to its detoxifying and antioxidative properties, and its immunostimulative and adsorption properties. Herein, we present the *in vitro* and *in vivo* study of clinoptilolite zeolite materials adsorption properties for D-glucose. In particular, we present data on the interaction of D-glucose on the tested zeolites' surface obtained by scanning electron microscope (SEM) and Energy-dispersive X-ray spectroscopy (EDS) and quantification by ultra high-performance liquid chromatography (UHPLC). We also present results on the reduction of blood glucose levels in mice pre-treated with clinoptilolite *in vivo* upon feeding with D-glucose. *In vivo* results were in line with the *in vitro* adsorption and/or interaction properties of tested zeolite materials for D-glucose and were quantified by UHPLC as well (11.34% for TMAZ; 10.82% for PMA and 8.76% for PMAO2). *In vivo* experiments in mice showed that PMA zeolite reduces blood glucose levels upon 15 min for 13% (at $p < 0.05$) up to 19.11% upon 120 min (without statistical significance) in clinoptilolite pre-treated mice fed by addition of D-glucose. Due to lack of explicit mechanistic knowledge on zeolite clinoptilolite interactions or adsorption with sugars *in vitro* and *in vivo*, presented study provides novel insights into these aspects for researchers in the field. The presented data merit further investigations as the material clearly shows a potential in management of hyperglycemia, such as for example in obese people, people with diabetes and people with metabolic syndrome where it could help regulate blood glucose levels.

Authors' contributions

RM performed sample preparation for the sugar-binding studies, participated in sugar-binding measurements, performed literature search, drafted corresponding parts of the manuscript; MF participated in sugar-binding studies and sample preparation for SEM; VS, IKP performed SEM and EDS measurements; SKP and DM conceptualized sugar-binding studies and prepared corresponding figures and tables, performed literature review; SKP drafted the manuscript and prepared tables; MJ performed HPLC measurements; KP and RS designed and visualized *in vivo* studies; RS performed *in vivo* studies; SKP and RM analyzed and interpreted the data; KP revised the final manuscript. All authors discussed results and agreed on the final manuscript version.

* Corresponding author.
E-mail address: sandrakp@uniri.hr (S. Kraljević Pavelić).
[1] Equal contribution.

https://doi.org/10.1016/j.cbi.2023.110641
Received 28 March 2023; Received in revised form 6 July 2023; Accepted 17 July 2023
Available online 22 July 2023

1. Introduction

The zeolite clinoptilolite is an aluminosilicate mineral of volcanic origin [1] built of silicon (SiO_4) and aluminum (AlO_4) tetrahedra that are bridged via one or more oxygen atoms. Its crystal framework contains intra-crystalline cavities and channels that are filled with cations and water. This stable crystal structure is essential for its physical and chemical properties including high water affinity and ion-exchange of polar molecules or ions [2]. Clinoptilolite zeolite material is also a molecular sieve with a large surface area. In particular silicates, alumosilicates and clinoptilolite have been previously shown to have immunostimulatory [3–5] and antioxidant [6] properties in living organisms as well as influence on protein and gene activities, i.e., signaling pathways [4,7,8]. As such, clinoptilolite zeolites are widely used in various fields and in biomedicine [8,9]. For example, zeolite-clinoptilolite has already been tested in clinical trials or in animals as an adjuvant in therapy for osteoporosis [10,11], in heavy metals detoxification effects studies [12–14], in athletes where it strengthened the intestinal wall integrity [15] or in wound healing applications [16]. These materials are interesting in other medical applications as well, for example as antimicrobial materials in stomatology [17] or as drug delivery systems [18].

For oral applications, clinoptilolite zeolite materials are mechanically or tribomechanically milled. These processes lead to a change in particle size and a significant increase in the specific surface area [19,20]. The ion exchange and adsorption properties of zeolite clinoptilolite are well-described and they include binding activities for heavy metals and lead (Pb), cadmium (Cd), arsenic (As), chromate (Cr), nickel (Ni), aluminum (Al) and ammonium (NH_4) cations [21–23].

Zeolite materials have excellent adsorption capacity for carbohydrates and are used in the sugar industry to adsorb and to separate sugars from aqueous solutions [24–26]. In these applications, different type of zeolite materials have been studied, the Faujasite type of zeolite, dealuminated β-zeolite, and a mixture of clinoptilolite-heulandite and mordenite zeolites. Each zeolite type bears specific physical-chemical properties and characterization of each material type prior to applications in industry or even medicine is a prerequisite a was, accordingly, subject of separate research. The impact and the use of zeolite adsorption for glycosides and their derivatives in living systems are however, less studied. Tribomechanically grounded nano-sized natural clinoptilolite material obtained under dynamic processing conditions which do not cause chemical changes in the raw materials, has however, already been proven as useful in the treatment of rats with type 1 diabetes [27] supporting a potential for clinoptilolite materials usage in certain pathologies or conditions in which sugar metabolism is impaired.

Thus, in this paper, we present experimental data obtained in the study of sugar binding and or interaction properties of the zeolite-clinoptilolite materials, having in mind a possible translational usage. In particular, the results of the *in vitro* study on the adsorption and or interaction properties of zeolite-clinoptilolite for D-glucose, as well as data of D-glucose levels in the blood of mice treated with zeolite-clinoptilolite materials using the *in vivo* glucose assay, are presented.

2. Material and methods

2.1. Materials and samples

The clinoptilolite materials TMAZ-zeolite (Tribo Mechanically Activated Zeolite, fine grinded and micronized raw zeolite material disclosed in patents HR P990263 A^2; US 2013/0119,174 A1; WO 2000/064,586 A1; DE 10200688 A1), PMA-zeolite material (Panaceo Micro Activation, registration according to the directive: European directive 93/42/EEC) and PMAO2-zeolite (Panaceo Micro Activation by Oxygenation) was kindly donated by Panaceo International Active Mineral Production GmbH, Austria. The clinoptilolite materials' chemical composition is provided in the Supplementary material (Supplementary material). Synthetic zeolite A (ZA) was from A. + E. Fischer-Chemie (Germany). Its chemical composition was: 46.73% SiO_2, 33.13%, Al_2O_3, 1.08%, Fe_2O_3, 16.36%, Na_2O. Characterization of materials used in this study has been published previously [22].

2.2. D-glucose adsorption studies

For adsorption studies ZA, TMAZ, PMA, and PMAO2 clinoptilolite zeolites' suspensions at 40 g/L zeolite in Milli-Q (mQ) water (H_2O) (pH = 7.18), model gastric solution (7 mL/L 37% HCl i 2 g/L NaCl; pH = 1.94) and model intestinal solution (8.649 g/L NaCl, pH = 5.7) were prepared. D-glucose solution (Sigma-Aldrich, USA) at 40 g/L of sugar in mQ H_2O prepared at room temperature was added to the zeolites' suspensions in mQ H_2O. All samples were vortexed for 1–2 min (Vortex 3 IKA, Germany), mixed for 30 min on the mixer (800 rpm; Electromagnetic mixer, IKA basic, Germany), room temperature, and incubated for 24 h in dark at room temperature. After 24 h incubation supernatant was separated from the precipitate and the supernatant was afterwards centrifuged at 4000 rpm (Centrifuge Eppendorf 5810 R, Germany) at 4 °C for 30 min. The mQ H_2O in all herein presented experiments was obtained using connected Ultrapure Water Systems (GenPure UV-TOC/UF xCAD plus) and Milli-Q water purification system (<0.055 μS/cm, Milli-Q Model Pacific TII 12; Thermo Fisher Scientific, Waltham, MA, USA).

The experimental design for adsorption studies was as follows:

Control 1: ZA, TMAZ, PMA, PMAO2 zeolites' suspensions (zeolites added in mQ H_2O at 40 g/L in mQ H_2O).

Control 2: tested D-glucose solution at 40 g/L in mQ H_2O

Test samples of ZA, TMAZ, PMA, PMAO2 zeolites' suspension + D-glucose solution.

2.2.1. Ultrahigh-performance liquid chromatography (UHPLC) analysis

The quantification of D-glucose, fructose, sucrose and lactose in the supernatants was performed by UHPLC chromatography. The analysis was performed on a liquid chromatograph instrument (Agilent 1260 Infinity II SFC/UHPLC Hybrid system, USA) with the column Hi-Plex Ca (Agilent Technologies, 8 μm, 300 mm × 7.7 mm, USA). mQ H_2O was used as a mobile phase. Flow 0,5 mL/min, analysis time 30 min, column temperature 85 °C, autosampler room temperature, detector RI 31 °C, injection volume 10 μL. Controls (mQ H_2O and D-glucose, fructose, sucrose and lactose solution set at concentration 2 mg/mL) and samples (mixed PMA-zeolite and D-glucose at 2 mg/mL supernatants obtained by centrifugation rate 4000 rpm) were injected into the instrument in duplicates. The calibration curve for D-glucose quantification was constructed by use of D-glucose solution in mQ H_2O at concentrations 2, 1.5, 1, 0.25, 0.125, 0.025 mg/mL.

2.3. Surface analysis by scanning electron microscopy (SEM) and energy dispersive X-ray spectroscopy (EDS)

Samples of zeolites in tested sugar D-glucose solutions were analyzed by the Scanning Electron Microscope QUANTA FEG 250 FEI, Low Vacuum SE detector (SEM) and EDS detector OXFORD PENTA FET (Thermo Fisher Scientific, USA). Each fraction of the obtained supernatants and precipitates in mQ H_2O were placed on carbon discs (carbon adhesive discs 12 mm, AGAR Scientific, UK) until complete drying. After 1 h, the dried samples were scanned by SEM using low vacuum detector and images were obtained in magnification range from 5000 to 20,000 in vacuum (100 Pa). To determine chemical composition of samples, EDS detector was employed. The ZA, TMAZ, PMA, PMAO2-zeolite enriched D-glucose samples prepared as described above were also analyzed by the same SEM instrument. Samples were again placed on carbon discs until complete drying and the same procedure as described above was applied for analysis.

Surface analyses of zeolites fractions in mQ H_2O, were done on the JEOL FE-SEM instrument (JSM-7800F PRIME, JEOL Ltd., Tokyo, Japan)

equipped with the EDS detector (X-MAX80 Aztec, Oxford instruments, UK). Zeolite particles were put on sample holder with carbon paste. Accelerating voltages for SEM and EDS were applied at 5 kV. For EDS measurements, 5 different places were selected to estimate reproducibility. Specifically, for material surface studies (SEM and EDS), suspensions of zeolites (ZA, TMAZ, PMA, PMAO2) were prepared by mixing each zeolite type in mQ H_2O. Samples were first decanted after 24 h incubation at room temperature and consequently centrifuged at 4000 rpm (Centrifuge Eppendorf 5810 R, Germany) at 4 °C for 30 min. The remaining supernatant was centrifuged again at 14,000 rpm (Centrifuge Eppendorf 5427 R, Germany) at 4 °C for 30 min and lastly at 140,000 rpm (Micro-ultracentrifuge, Thermo Fisher Scientific, Germany) at 4 °C for 30 min. All obtained precipitates and supernatants were analyzed by SEM and EDS.

2.4. Oral D-glucose test in vivo

The *in vivo* experiments were performed on C57BL/6 Zgr/Hr female mice. Animals were 3–4 months old at the beginning of the experiments. Six mice were used in each group per experiment. Mice were obtained from Rudjer Boskovic Institute's breeding colony. During the experimental period, six animals were kept per cage. The bottoms of the cages were covered with sawdust (Scobis Uno®, Mucedola srl, Italy). Standard food for laboratory mice (4RF 21 GLP® Mucedola srl, Italy) was used. Access to food and water was ad libitum. Animals were kept in conventional circumstances: light/dark rhythms of 12/12 h, temperature of 22 °C, and humidity of 55%. All experiments were performed according to the Institute for Laboratory Animal Research - ILAR Guide for the Care and Use of Laboratory Animals, EU Directive 2010/63/EU, and Croatian animal protection law (NN 102/17). All procedures performed on animals have been approved by the Ethics Committee of the Ministry of Agriculture and Forestry of the Republic of Croatia – UP/I-322-01/21–01/49. An oral D-glucose tolerance test (OGTT) or glucose load test was performed according to the following design:

1. Negative control
2. Positive control 1 – PMA zeolite 4 g/kg
3. Positive control 2 – D-glucose solution 2 g/kg
4. Protocol 1 – Treatment of PMA zeolite 4 g/kg daily for 3 days and 24 h after the last administration of PMA D-glucose solution 2 g/kg
5. Protocol 2 – application of D-glucose solution 2 g/kg + PMA zeolite 4 g/kg simultaneously

Freshly prepared solutions of D-glucose and suspensions of PMA zeolite in sterile water were used in the experiments. The required concentration of test compounds was dissolved/suspended in 10 mL/kg body weight of mice. Before D-glucose administration, mice have fasted for 12 h. Blood was sampled from the lateral tail vein using a lancet. Baseline D-glucose levels were measured using a Start Strip Xpress (Nova Biomedical) glucometer. D-Glucose was then administered and its level in the blood was determined at time points of 15, 30, 60 and 120 min after application, using the methodology described for determining basal glucose concentration. The animals were then anaesthetized using 3% isoflurane. After it was confirmed that the animal is under deep anesthesia (bradycardia, absence of palpebral and corneal reflex), the animals were sacrificed by cutting the jugular vein to take the necessary blood, which was used for further qualitative and quantitative biochemical tests at 10 μl on EDTA for the whole blood analysis and at 100 μl of whole blood for Heparin liver tests. The whole blood tests were done on Auto Hematology Analyzer BC-30 Vetfor (Mindray, Shenzhen China): white blood cell (WBC); red blood cell (RBC); hemoglobin (HB); hematocrit (HCT); mean corpuscular volume (MCV); mean corpuscular hemoglobin (MCH); mean corpuscular hemoglobin concentration (MCHC); platelet crit (PCT); red cell distribution width (RWD). Liver tests were done on RC clinical chemistry analyzer with comprehensive rotor (Scil Animal Care Company, Germany) with heparin as follows: alanine aminotransferase (ALT); albumin (ALB); alkaline phosphatase (ALP); amylase (AMY); gamma glutamyltransferase (GGT); D-glucose (Glu); creatinine (CREA); globulin (Glob); tbilirubin (TBIL); urea (BUN); albumin/globulin ratio (A/G); phosphates (PHOS); total proteins (TP); total cholesterol (TC).

2.4.1. Statistical analysis

The results from the *in vivo* studies were statistically analyzed by the multiple Mann Whitney U-nonparametric test, followed by the Kruskal Wallis, ANOVA, test at significance level $p > 0.05$ (Program Sigma Stat v. 3.5).

3. Results

3.1. Synthetic zeolite A and clinoptilolite zeolites TMAZ, PMA, and PMAO2 surface study by SEM and EDS

For the surface analysis of tested zeolite materials (ZA, TMAZ, PMA, PMAO2) from mQ H_2O suspension fractions (decanted fraction, and fractions upon centrifugation at 4000 rpm, 14,000 rpm and 140,000 rpm), scanning electronic microscopy (SEM) was used in combination with elemental analysis EDS. For the elemental analysis we measured and consequently compared the average mass percentages values for the following elements: Si, O, C, Na and Al. The results were compared with elemental analysis of the corresponding solid dry zeolites (ZA, TMAZ, PMA, PMAO2). The appearance of tested materials conformed with previously observed forms and shapes [22] and are depicted in Supplementary Figs. 1–4. Particle size information is also provided in Supplementary Table 6. EDS analysis (Table 1), shows a clear pattern of surface dissolving processes in mQ H_2O as witnessed by formation of new crystal structures observed in fractions upon centrifugation where silicon structures dominated in the clinoptilolite supernatants (Supplementary Fig. 2, panels B,C,D; Supplementary Fig. 3, panels B,C,D; Supplementary Fig. 4, panel B,C,D). Moreover, the Si/Al ratio of the tested zeolites' surface in the decanted fractions calculated from EDS analysis was: for ZA 0.94 which is similar to the solid ZA Si/Al ratio = 1.41 (Supplementary Table 5) and for TMAZ = 6.45; PMA = 6.86 and for PMAO2 = 7.33 which is expectedly similar to the solid materials (Si/Al = 6.25–6.98). However, the Si content increased drastically in supernatants after centrifugation at 4000 rpm confirming the presence of Si species released from the material into water. The average values for Si/Al ratio of these formed structures were: ZA 30.84, TMAZ 86.98, PMA 81.71 and PMAO2 34.05 (Supplementary Table 5). Formed amorphous Si forms in the zeolites' water suspensions were clearly visible by SEM. In addition to the small zeolite particles and amorphous silicon forms observed with SEM, Al-containing particles were also released from the zeolite surface upon centrifugation, particularly from the ZA (Table 1).

Average values of elements C and Na increased upon repeated centrifugation probably due to release of Na + cations from the zeolite structure and carbon gasses from the zeolite pores as a consequence of applied centrifugal force.

3.2. Synthetic zeolite A and clinoptilolite zeolites TMAZ, PMA, and PMAO2 adsorption and/or interaction properties for D-glucose in vitro

D-Glucose adsorption and/or interaction on the tested zeolites' surfaces was evaluated through measurement of carbon percentage changes on the zeolite materials surfaces' as in the solid forms of tested zeolites no carbon atoms were detected. This zeolite composition was also corroborated by the declaration issued by the manufacturer (Supplementary material). The surface appearance of tested zeolites in D-glucose solution is presented on Figs. 1–8 (Figs. 1–8).

In particular, on Figs. 1–4, panels A, the surface appearance of the tested zeolite materials is presented without addition of D-glucose. On Figs. 1–4-, panels B, formation of a hydrogel-type formation in the supernatant of zeolite D-glucose suspension was expectedly observed for

Table 1
Elemental analysis (EDS) of tested zeolites' surface (Zeolite A, TMAZ, PMA and PMAO2) decanted suspensions and supernatants upon centrifugation at 4000, 14,000, 140,000 rpm. Si – silicon, O – oxygen, C – carbon, Na – sodium, Al – aluminum. Solid material data is reported from declarations accompanying the tested materials.

Material	Fraction	Element presence in percentages (wt %)				
		Si	O	C	Na	Al
Zeolite A	Decanted fraction	16.00	49.35	2.70	15.33	16.62
	4000 rpm fraction	16.00	38.60	14.21	29.79	1.40
	14,000 rpm fraction	16.96	35.91	13.34	33.57	0.22
	140,000 rpm fraction	12.00	37.85	15.60	31.36	2.91
	Solid material (Si, Na, Al as oxides)	46.73		/	16.36	33.13
TMAZ	Decanted fraction	37.45	49.70	3.05	4.00	5.80
	4000 rpm fraction	46.23	27.90	10.50	16.64	0.73
	14,000 rpm fraction	26.20	29.31	13.78	30.00	0.55
	140,000 rpm fraction	15.00	40.36	12.30	32.20	0.10
	Solid material (Si, Na, Al as oxides)	65.00–71.30		/	0.20–1.30	9.30–11.40
PMA	Decanted fraction	39.83	47.70	2.46	4.21	5.80
	4000 rpm fraction	40.66	36.61	11.08	10.79	0.86
	14,000 rpm fraction	36.11	33.88	19.22	9.62	1.17
	140,000 rpm fraction	45.15	26.65	11.21	16.72	0.27
	Solid material (Si, Na, Al as oxides)	65.00–71.30		/	0.20–1.30	9.30–11.40
PMAO2	Decanted fraction	41.10	42.20	9.10	2.00	5.60
	4000 rpm fraction	33,04	34.29	9.80	21.59	1.28
	14,000 rpm fraction	37.55	32.64	10.21	18.38	1.22
	140,000 rpm fraction	29.63	35,76	11.26	22.70	0.65
	Solid material (Si, Na, Al as oxides)	65.00–71.30		/	0.20–1.30	9.30–11.40

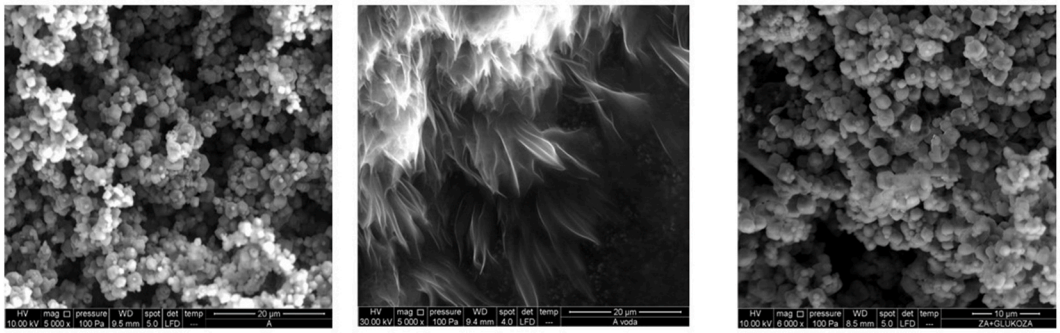

Fig. 1. SEM images of the solid Zeolite A (Panel A), supernatant upon 4000 rpm centrifugation of the zeolite suspension in D-glucose solution at 40 g/L (panel B) and the precipitate upon 4000 rpm centrifugation of the zeolite suspension in D glucose solution at 40 g/L (Panel C). The images were obtained by Scanning Electron Microscope SEM QUANTA FEG 250 FEI, Low Vacuum SE detector (Thermo Fischer Scientific, USA). Magnification 5000x or 6000x.

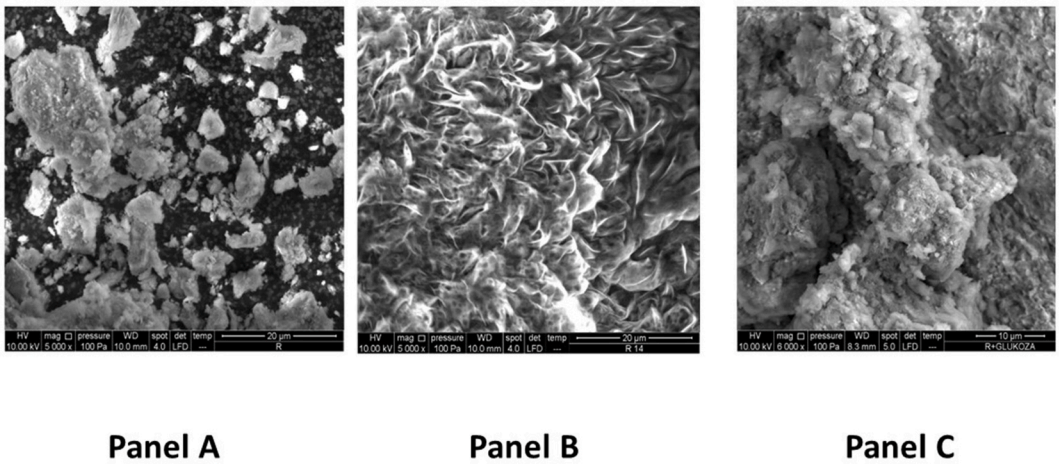

Fig. 2. SEM images of the solid TMAZ (Panel A), supernatant upon 4000 rpm centrifugation of the zeolite suspension in D-glucose solution at 40 g/L (panel B) and the precipitate upon 4000 rpm centrifugation of the zeolite suspension in D-glucose solution at 40 g/L (Panel C). The images were obtained by Scanning Electron Microscope SEM QUANTA FEG 250 FEI, Low Vacuum SE detector (Thermo Fischer Scientific, USA). Magnification 5000x or 6000x.

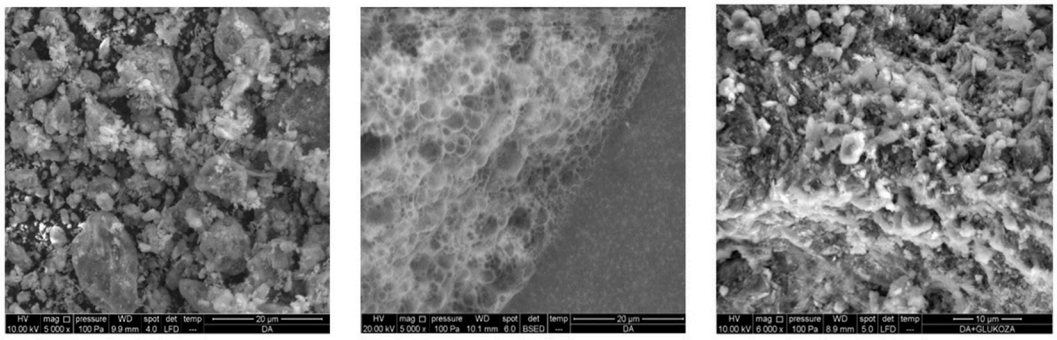

Fig. 3. SEM images of the solid PMA (Panel A), supernatant upon 4000 rpm centrifugation of the zeolite suspension in D-glucose solution at 40 g/L (panel B) and the precipitate upon 4000 rpm centrifugation of the zeolite suspension in D-glucose solution at 40 g/L (Panel C). The images were obtained by Scanning Electron Microscope SEM QUANTA FEG 250 FEI, Low Vacuum SE detector (Thermo Fischer Scientific, USA). Magnification 5000x or 6000x.

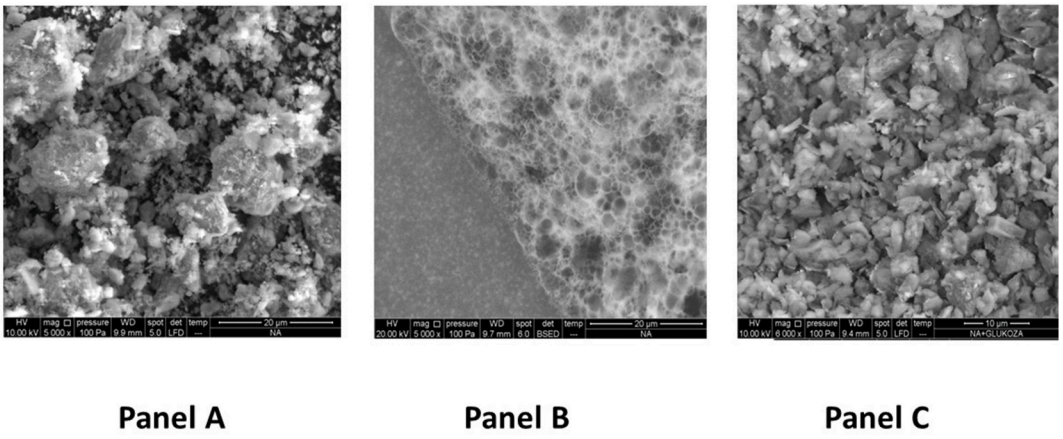

Fig. 4. **S**EM images of the solid PMAO2 (Panel A), supernatant upon 4000 rpm centrifugation of the zeolite suspension in D-glucose solution at 40 g/L (panel B) and the precipitate upon 4000 rpm centrifugation of the zeolite suspension in D-glucose solution at 40 g/L (Panel C). The images were obtained by Scanning Electron Microscope SEM QUANTA FEG 250 FEI, Low Vacuum SE detector (Thermo Fischer Scientific, USA). Magnification 5000x or 6000x.

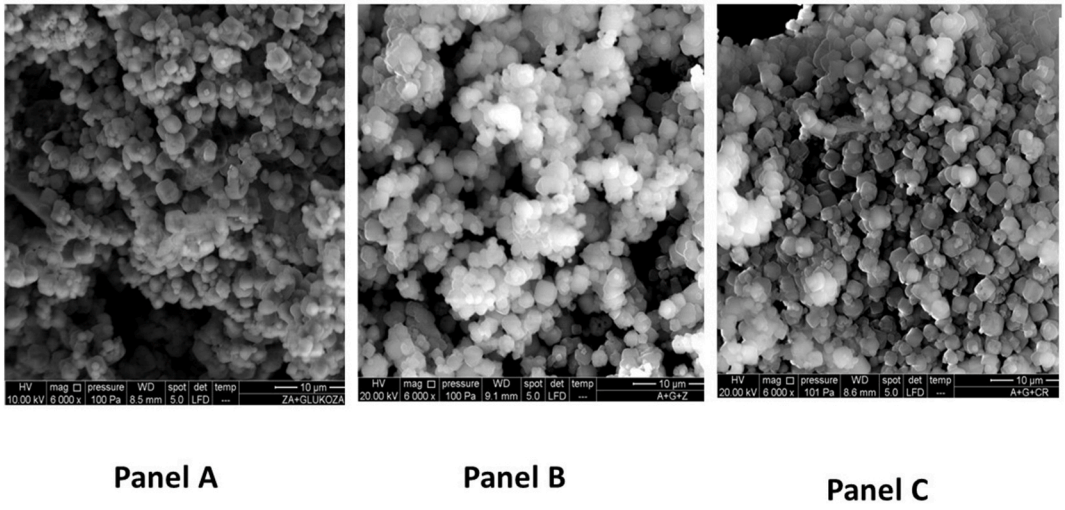

Fig. 5. SEM images of the Zeolite A precipitate upon 4000 rpm centrifugation of the zeolite suspension in D-glucose solution at 40 g/L in water (Panel A), in the gastric model solution (pH = 1.94) (panel B) and intestinal model solution (pH = 5.7) (Panel C). The images were obtained by Scanning Electron Microscope SEM QUANTA FEG 250 FEI, Low Vacuum SE detector (Thermo Fischer Scientific, USA). Magnification 6000x.

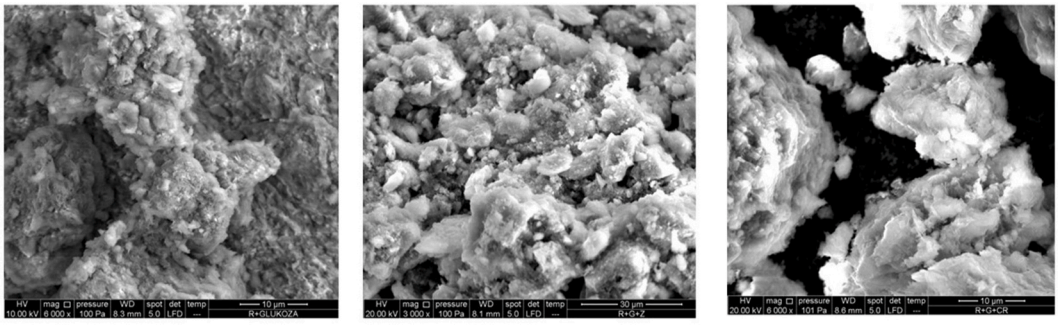

Fig. 6. SEM images of the TMAZ precipitate upon 4000 rpm centrifugation of the zeolite suspension in D-glucose solution at 40 g/L in water (Panel A), in the gastric model solution (pH = 1.94) (panel B) and intestinal model solution (pH = 5.7) (Panel C). The images were obtained by Scanning Electron Microscope SEM QUANTA FEG 250 FEI, Low Vacuum SE detector (Thermo Fischer Scientific, USA). Magnification 3000x or 6000x.

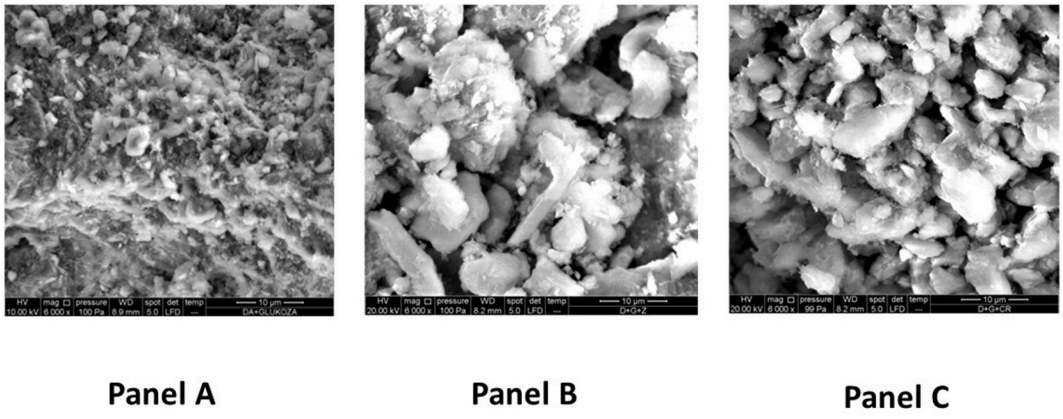

Fig. 7. SEM images of the PMA precipitate upon 4000 rpm centrifugation of the zeolite suspension in D-glucose solution at 40 g/L in water (Panel A), in the gastric model solution (pH = 1.94) (panel B) and intestinal model solution (pH = 5.7) (Panel C). The images were obtained by Scanning Electron Microscope SEM QUANTA FEG 250 FEI, Low Vacuum SE detector (Thermo Fischer Scientific, USA). Magnification 6000x.

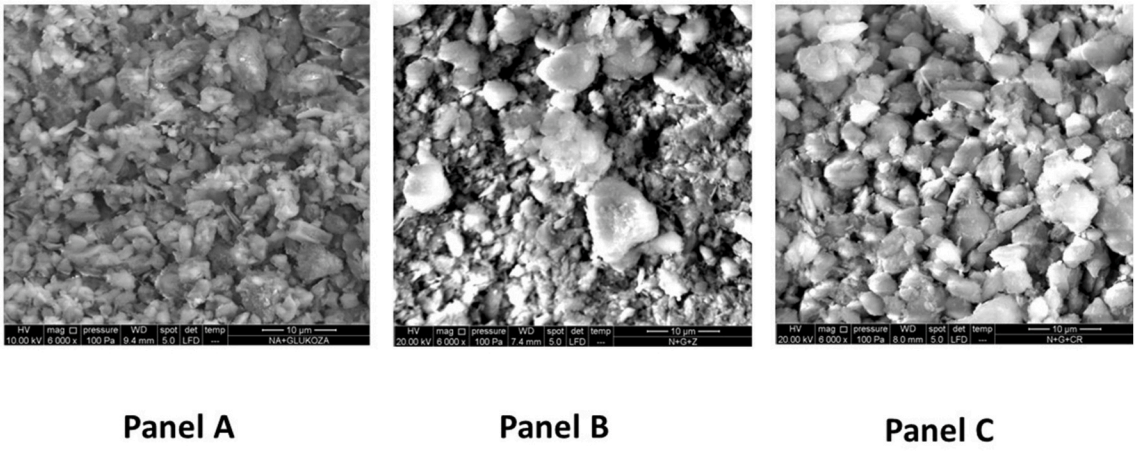

Fig. 8. SEM images of the PMAO2 precipitate upon 4000 rpm centrifugation of the zeolite suspension in D-glucose solution at 40 g/L in water (Panel A), in the gastric model solution (pH = 1.94) (panel B) and intestinal model solution (pH = 5.7) (Panel C). The images were obtained by Scanning Electron Microscope SEM QUANTA FEG 250 FEI, Low Vacuum SE detector (Thermo Fischer Scientific, USA). Magnification 6000x.

all materials, which may be assigned to formations of D-glucose hydrogel-like forms or thin layers and confirmed as increased carbon quantity by EDS analysis of these formations (Table 3). To prove adsorption and/or interaction of D-glucose on the zeolite materials' surface, D-glucose solution containing tested zeolite materials was subjected to centrifugation at 4000 rpm and on Figs. 1–4, panels C, adsorption and/or interaction of D-glucose was not or only barely visible as a layer on the surface of the zeolites, but was confirmed as increased

Table 2
Elemental analysis (EDS) of the tested zeolites' precipitates (Zeolite A, TMAZ, PMA and PMAO2) from glucose solution at 40 g/L upon centrifugation at 4000 rpm. Si – silicon, O – oxygen, C – carbon, Na – sodium, Al – aluminum. The results are presented in comparison with elemental analysis of the solid material of tested zeolites. Solid material data is reported from declarations accompanying the tested materials.

Material	Fraction	Element presence in percentages (wt %)				
		Si	O	C	Na	Al
Zeolite A + d-glucose precipitate	4000 rpm fraction	4.21	45.09	41.04	4.69	4.97
Zeolite A	solid material	46.73		/	16.36	33.13
TMAZ + d-glucose precipitate	4000 rpm fraction	14.75	47.40	33.04	/	2.68
TMAZ	solid material	65.00–71.30		/	0.20–1.30	9.3–11.4
PMA + d-glucose precipitate	4000 rpm fraction	14.77	43.98	35.18	/	2.7
PMA	solid material	65.00–71.30		/	0.20–1.30	9.30–11.40
PMAO2 + d-glucose precipitate	4000 rpm fraction	15.91	45.13	32.46	/	3.02
PMAO2	solid material	65.00–71.30		/	0.2–1.3	9.30–11.40

Table 3
Elemental analysis (EDS) of tested zeolites' (Zeolite A, TMAZ, PMA and PMAO2) supernatants obtained upon 4000 rpm centrifugation of the zeolites solutions with D-glucose at 40 g/L in. Si – silicon, O – oxygen, C – carbon, Na – sodium, Al – aluminum. The results are presented in comparison with elemental analysis of zeolites and glucose solution in mQ H_2O.

Material	Element presence in percentages (wt %)				
	Si	O	C	Na	Al
Zeolite A + d-glucose	0.08	51.48	48.13	0.17	/
Zeolite A + mQ H_2O	16.00	38.60	14.21	29.79	1.40
TMAZ + d-glucose	0.12	35.89	62.99	0.22	0.48
TMAZ + mQ H_2O	46.23	27.90	10.50	16.64	0.73
PMA + d-glucose	0.05	34.79	64.17	0.52	/
PMA + mQ H_2O	40.66	36.61	11.,08	10.79	0.86
PMAO2 + d-glucose	0.30	43.79	55.24	0.19	/
PMAO2 + mQ H_2O	33.04	34.29	9.80	21.59	1.28

carbon quantity by EDS analysis (Table 2).

A thin layer of D-glucose is also not or scarcely visible on the zeolites' surface in the acidic D-glucose solutions (gastric and intestinal pH model solution) as well (Figs. 5–8), but was confirmed as increased carbon quantity by EDS analysis (Table 4). Accordingly, we may corroborate the adsorption and/or interaction of D-glucose on zeolite surface in the intestine *in vivo* conditions as well. This possibility should be however, additionally tested in more complex intestinal model solutions.

The precipitate of synthetic ZA after 24 h-incubation with D-glucose and upon centrifugation at 4000 rpm had 41.04% C on the material surface, while in the case of natural zeolite clinoptilolite the C percentage was for 33.04% TMAZ, 35.18% for PMA, and 32.46% for PMAO2 (Table 2). Interestingly, in comparison with results of the supernatants obtained from zeolite materials' suspensions in mQ H_2O where the percentage of Na^+-ions was increased upon centrifugation (Table 3), in D-glucose zeolite solutions Na^+ was not detected after centrifugation. This is probably due to changes of the zeolite surface in D-glucose solution that might include formation of a thin sugar layer, which might have prevented the ion-exchange process with the environment occurring between zeolite pores and channels containing diverse cations, including the measured Na^+.

In contrast to Zeolite A that adsorbed and/or interacted with D-glucose up to 34.46% witnessed by measurement of C on the surface (Table 4), natural clinoptilolite materials adsorbed and/or interacted with D-glucose at a higher rate in the acidic model gastric and intestinal solutions. For example, in the intestinal model solution (pH = 57) the percentage of C was accordingly for TMAZ 5102%, PMA 6785% and PMAO2 6511% (Table 4). These percentages were higher than the percentages measured for zeolites TMAZ, PMA, PMAO2 in the D-glucose mQ water solution. In the gastric model solution, the elemental analysis for C was not obtained which may be the consequence of high Si and Al release from the surface of the material in the very low pH (pH = 194) (Table 4).

3.3. Adsorption quantification of D-glucose interaction with the synthetic zeolite A and clinoptilolite zeolites TMAZ, PMA, and PMAO2 by use of UHPLC

D-Glucose adsorption and/or interaction on synthetic ZA, and clinoptilolite materials TMAZ, PMA and PMAO2- was additionally validated and quantified by UHPLC (Table 5). The results of UHPLC analysis showed that the concentration of D-glucose in the ZA D-glucose enriched solution was diminished by 11.85%, the concentration of D-glucose in the TMAZ-zeolite D-glucose enriched solution was diminished by 11.34%, concentration of D-glucose in the PMA-zeolite D-glucose enriched solution was diminished by 10.82% and the concentration of D-

Table 4
Elemental analysis (EDS) of the tested zeolites (zeolite A, TMAZ, PMA and PMAO2) precipitates upon centrifugation at 4000 rpm from the **D-glucose** solution (40 g/L) in water, model gastric (pH = 194) and intestinal solutions (pH = 57). Si – silicon, O – oxygen, C – carbon, Na – sodium, Al – aluminum. The results are presented in comparison with elemental analysis of zeolites and glucose solution in mQ H_2O.

Material	Element presence in percentages (wt %)				
	Si	O	C	Na	Al
Zeolite A + d-glucose in mQ H_2O	4.21	45.09	41.04	4.69	4.97
Zeolite A + d-glucose in gastric model solution	7.45	50.20	26.83	6.81	8.71
Zeolite A + d-glucose in intestinal model solution	5.77	46.68	34.46	6.36	6.63
TMAZ + d-glucose in mQ H_2O	14.75	47.40	33.04	/	2.68
TMAZ + d-glucose in gastric model solution	23.28	62.60	/		5.29
TMAZ + d-glucose in intestinal model solution	7.87	37.74	51.02	0.75	1.46
PMA + d-glucose in mQ H_2O	14.77	43.98	35.18	/	2.70
PMA + d-glucose in gastric model solution	2.11	33.61	62.43	/	0.43
PMA + d-glucose in intestinal model solution	1.71	27.35	67.85	/	0.54
PMAO2 + d-glucose in mQ H_2O	15.91	45.13	32.46	/	3.02
PMAO2 + d-glucose in gastric model solution	17.52	60.01	/	/	14.20
PMAO2 + d-glucose in intestinal model solution	1.33	27.61	65.11	/	1.83

Table 5
UHPLC results and quantification of D-glucose. The results were obtained for zeolites ZA, TMAZ, PMA, PMAO2 D-glucose solutions after centrifugation at 4000 rpm and are presented as D-glucose concentrations in mg/ml. Control: D-glucose solution at 2 mg/mL. Calibration curve for tested glucose was constructed for the concentration range 2, 1.5, 1, 0.25, 0.125 and 0.025 mg/mL.

Sample	Concentration (mg/ml)
d-Glucose standard in mQ H_2O	1.94
Zeolite A suspension with **d**-glucose	1.71
Δ value (%)	**11.85%**
d-glucose standard in mQ H_2O	1.94
Zeolite TMAZ suspension with **d**-glucose	1.72
Δ value (%)	**11.34%**
d-Glucose standard in mQ H_2O	1.94
Zeolite PMA suspension with **d**-glucose	1.73
Δ value (%)	**10.82%**
d-glucose standard in mQ H_2O	1.94
Zeolite PMAO2 suspension with **d**-glucose	1.77
Δ value (%)	**8.76%**

glucose in the PMAO2-zeolite D-glucose enriched solution was diminished by 8.76% in comparison with control solution of D-glucose without zeolites (Table 5).

3.4. *In vivo studies on mice pre-treated with PMA zeolites and fed with the addition of D-glucose*

The *in vivo* validation of *in vitro* observed D-glucose adsorption and/or interaction on the tested zeolites materials was performed for PMA as this material is a registered EU medical device for use in humans. At the day of blood glucose testing, animals were administered with D-glucose at the following regimen: co-administration of D-glucose with PMA or pre-treatment with PMA 3-days in raw before D-glucose administration. Controls groups were negative control (no treatment), PMA-treated mice and D-glucose-treated mice. D-Glucose was measured in the blood of animals (mmol/L) 15, 30, 60 and 120 min upon corresponding treatments. The results show a decrease in glucose levels in PMA-pretreated and PMA-treated animals' groups upon 15 and 30 min of D-glucose administration in comparison to glucose-only treated animals (Fig. 9). The decrease was comparable to UHPLC results in previously performed *in vitro* testing, where D-glucose was adsorbed by PMA up to 10.82%. Accordingly, in the *in vivo* experiment 13% of D-glucose levels were decreased in PMA-treated animal blood upon glucose administration after 15 min and 18% in PMA-treated animal blood upon glucose administration after 30 min without statistical significance. Similarly, 15% of D-glucose levels were decreased in PMA-pretreated animals' blood upon glucose administration after 15 min (at $p > 0.001$) and 14% in PMA-pretreated animal blood upon glucose administration after 30 min without statistical significance. The relevant biochemical parameters were not altered by PMA-treatment. Albumin to globulin ratio, amylase and total proteins were altered by D-glucose treatment (Supplementary Table 3).

4. Discussion

Zeolites exhibit unique adsorption and ion-exchange properties due to their porous cation-filled aluminosilicate crystal structure and large surface area. The ion exchange properties of zeolites are based on the presence of exchangeable cations in the pores and cavities bound to the aluminosilicate crystal lattice by weak electrostatic bonds, which allows their mobility into and out of the zeolite structure, resulting in the ion exchange with cations from the environment in a stoichiometric ratio [28,29]. In addition, the adsorption properties of zeolites are based on the Brønsted-Lewis theory according to which there are acidic and alkaline sites in the zeolite structure. According to this theory, the oxygen atom in the aluminosilicate structure of zeolite (≡ Si–*O*–Al ≡) is a proton acceptor, has a negative charge and represents a potential adsorption site for positive ions or polar organic molecules [30]. In our study, we first studied the changes in zeolite surface in mQ H_2O that led to the release of Si-forms into the environment. Soluble Si-forms released from the zeolite surface in water, form various polymers with high affinity for Al-species in a chemical equilibrium reaction in water [31]. In the same way, the solid zeolite structure that releases Si-forms in water environment, also retains the high affinity for Al-forms from the environment. This change in the composition of the zeolite surface in the centrifuged fractions analyzed herein, was evidenced by the EDS analysis and by the changed ratio of Si/Al in the centrifuged fractions of the zeolite materials. This Si/Al ratio increased several times in the centrifuged fractions, confirming the presence of Si-forms in the solutions. The scanned crystal shapes of the centrifuged fractions had a completely

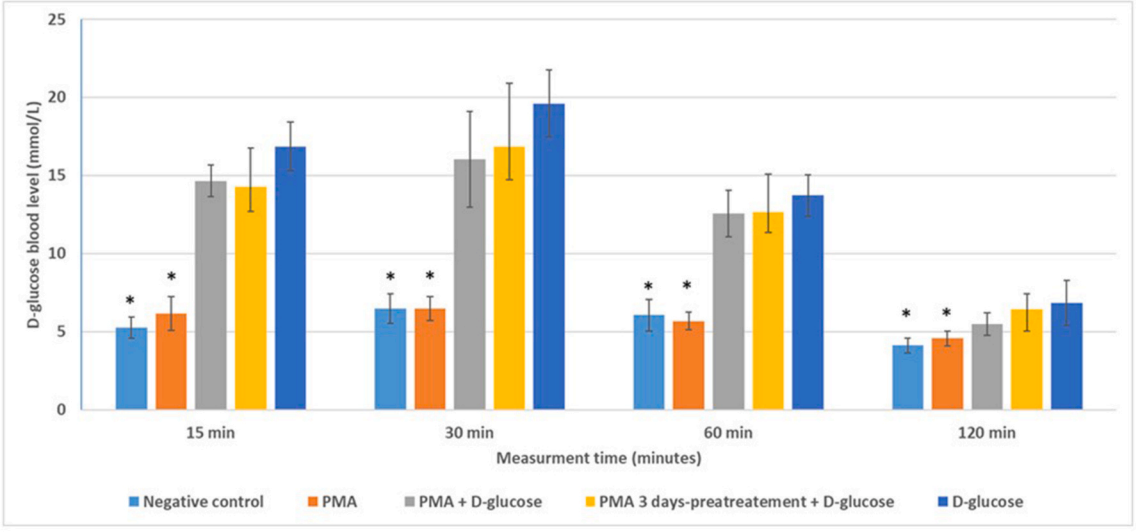

Fig. 9. D-glucose levels in mice blood measured in mmol/L in animals administered with glucose pre-treated for 3 days with PMA or administered concomitantly with PMA and D-glucose. D-glucose blood levels were measured after 15, 30, 60 and 120 min upon glucose administration. Statistically relevant differences between animal groups were shown with an asterisk (*) in comparison with D-glucose group (at $p > 0.05$). Groups: negative control – healthy, untreated animals; PMA – daily PMA treated animals until the day of blood glucose testing; PMA + D-glucose – animals administered with PMA and D-glucose concomitantly at the day of blood glucose testing; PMA pre-treated group for 3 days before administration of D-glucose at the day of blood glucose testing; D-glucose - animals treated with D-glucose at the day of blood glucose testing.

different shape than the zeolite materials observed by SEM in the decanted fractions as the main material zeolite fraction was removed by decantation and only small zeolite particles factions or newly formed Si or Al particles remained in centrifuged fractions. The zeolite particles in the decanted fractions on the other side, as expected, reflect the shape and content of zeolite materials in the solid state. Further on, the clinoptilolite zeolites might have good adsorption properties for glycosides from water due to the presence of active oxygen atoms on the surface, which can bind hydroxyl and aldehyde groups from sugars. In our study we also documented a good affinity of tested natural clinoptilolite materials TMAZ, PMA and PMAO2 towards D-glucose in mQ H_2O. This affinity was significantly higher in the intestinal model solutions with acidic pH, probably because the oxygen atom in the zeolite structure is a proton acceptor. For example, the percentage of measured carbon indicating the presence of D-glucose on the surface of zeolite materials that were precipitated before and after centrifugation at 4000 rpm, was increased in samples obtained from intestinal model solutions (17.98% for TMAZ, 32.69% for PMA and for 32.65% for PMAO2) in comparison with mQ H_2O solutions. This affinity for D-glucose adsorption and/or interaction was confirmed and quantified by liquid chromatography (UHPLC). Still, the exact mechanism of zeolite surface interaction with D-glucose that might include direct adsorption, binding or interaction through formation of D-glucose thin layer around zeolite surface, should be studied in more details with additional methods and tests.

The observed property can be exploited in the *in vivo* systems, as glucose levels and oxidative stress were already found to be reduced in rats with type 1 diabetes after application of a nanosized clinoptilolite material [27]. In this study, the authors applied a nano-sized material, while the material tested in our study was a micronized material with a diameter range from 1.2 μm to 24.2 μm (Supplementary material). Moreover, the authors studied the effects of the nanosized clinoptilolite material in a diabetic rat model while in our study we tested the effects of PMA on glucose blood levels of healthy mice. The nanosized clinoptilolite material proved to decrease blood glucose levels in diabetic rats to near normal levels. Accordingly, our results cannot be directly comparable with this study and bring specific relevance for preventive applications in physiological conditions. Moreover, zeolite nanoparticles may directly enter into the circulation while PMA employed in our study does not enter into circulation, as proven in our previous studies [14]. In addition, lowering of blood glucose levels in mice fed with D-glucose in our study occurred with statistical significance only in the group pretreated with PMA for 3 days. This implies additional mechanisms of action, that probably include some effects on the intestinal status and the gut microbiome that merit further research as well.

Moreover, from a biological point of view, glucose levels in the blood are regulated by homeostatic mechanisms [32] which is of key importance for health. However, in a number of diseases, such as diabetes, or metabolic syndrome, the blood glucose levels are deregulated [33]. In such patients, various strict dietary and pharmacological interventions are required, resulting in a decreased quality of life. Integrative approaches, including usage of less invasive treatments based on natural compounds such as for example vitamins [34] or, as suggested herein, the zeolite clinoptilolite materials alone or as drug carriers [35] can be therefore evaluated as a possible dietary intervention that can help regulate glucose blood levels. In particular, our results confirmed the efficacy of the tested clinoptilolite material PMA, in mice in reducing blood glucose levels for 13% in 15 min–18% in 30 min. Compared to cinnamon, for example, the efficiency of zeolite was higher in our study. Cinnamon lowered blood glucose levels on average at days 20 and 40, by 4.17% and 4.90% at 1 g of cinnamon per day, by 1.84% and 2.75% at 3 g of cinnamon per day, and by 4.55% and 5.92% at 6 g of cinnamon per day [36]. Kazuhiro et al. recently demonstrated the usefulness of adding natural zeolite to the mice diet in a model mouse with high-fat-induced obesity and type 2 diabetes mellitus. The addition of zeolite at 10% within the regular diet stopped weight gain and lowered plasma triacylglycerol, total cholesterol and high-density-lipoprotein cholesterol levels as well as fasting blood glucose levels. Similar to our study, postprandial blood glucose levels were reduced with zeolite ingestion in an oral glucose tolerance test at week 12 [37]. Pavelic and Hadžija also reported the observed adsorption of glucose by zeolite and the observed beneficial effects of zeolite clinoptilolite in diabetic mice [38]. They suggest that silica released from zeolites *in vivo*, may also play a role in this process, as it has previously been shown that silica supplementation can completely prevent spontaneous diabetes in BB mice [39].

The data presented here provide further evidence for clinoptilolite zeolite materials usage in management of D-glucose in individuals with impaired glucose metabolism or diabetes. This field of application for clinoptilolite zeolite materials is particularly interesting in the context of a growing interest in the integrative medicine approaches that are based on oral interventions with different natural compounds, nutraceuticals and plant extracts due to high biocompatibility and no, or very low toxicity that might be further studied as a support to the standard therapy protocols [40–46].

5. Conclusions

The clinoptilolite zeolite material interactions with D-glucose described *in vitro* and validated *in vivo* in mice, merit further research as lowering of D-glucose concentrations in solutions with zeolite clinoptilolite materials *in vitro* and lowering of blood glucose levels were observed in mice fed with D-glucose at statistical significance in the group pretreated with PMA zeolite for 3 days. The observed *in vivo* effect also suggests that mechanisms other than adsorption are relevant for glucose uptake and occur after ingestion of clinoptilolite zeolite material in the intestine. The presented study provides novel insights into sugar-zeolite clinoptilolite interactions for researchers in the field. The presented data merit further investigations as the material clearly shows a potential in management of hyperglycemia, such as for example in obese people, people with diabetes and people with metabolic syndrome where it could help regulate blood glucose levels. Further investigations of the observed phenomena are also needed for reaching of definite conclusions on the mechanisms underlying observed *in vitro* and *in vivo* phenomena. At last, it is important to state that the material quality and chemical composition of the zeolite clinoptilolite materials are a prerequisite for *in vivo* applications.

Funding

The study was funded by the University of Rijeka research support grant uniri-biomed-18-150 given to SKP. Additional funding has been provided by the Croatian government and the European Union (European Regional Development Fund—the Competitiveness and Cohesion Operational Program—KK.01.1.1.01) through the Bioprospecting of the Adriatic Sea project (KK.01.1.1.01.0002) granted to The Scientific Centre of Excellence for Marine Bioprospecting-BioProCro.

Institutional review board statement

All experiments on animals were performed according to the ILAR Guide for the Care and Use of Laboratory Animals, EU Directive 2010/63/EU, and Croatian animal protection law (NN 102/17). All procedures performed on animals have been approved by the Ethics Committee of the Ministry of Agriculture and Forestry of the Republic of Croatia – UP/I-322-01/21–01/49.

Informed consent statement

Not applicable.

Declaration of competing interest

The authors declare that they have no known competing financial

interests or personal relationships that could have appeared to influence the work reported in this paper.

Data availability

All data is presented in the Manuscript and accompaining Supplementary material

Acknowledgments

We acknowledge Dr. Marin Roje for help in UHPLC studies and Dr. Tihomir Balog for assisting the biochemical blood measurements.

Appendix A. Supplementary data

Supplementary data to this article can be found online at https://doi.org/10.1016/j.cbi.2023.110641.

References

[1] F.A. Mumpton, La roca magica: uses of natural zeolites in agriculture and industry, Proc. Natl. Acad. Sci. U. S. A. 96 (7) (1999) 3463–3470, https://doi.org/10.1073/pnas.96.7.3463.
[2] C. Laurino, B. Palmieri, Zeolite: "the magic stone"; main nutritional, environmental, experimental and clinical fields of application, Nutr. Hosp. 32 (2015) 573–581, https://doi.org/10.3305/nh.2015.32.2.8914.
[3] T. Aikoh, A. Tomokuni, T. Matsukii, F. Hyodoh, H. Ueki, T. Otsuki, A. Ueki, Activation-induced cell death in human peripheral blood lymphocytes after stimulation with silicate *in vitro*, Int. J. Oncol. 12 (6) (1998) 1355–1359, https://doi.org/10.3892/ijo.12.6.1355.PMID:9592199.
[4] K. Pavelić, M. Hadzija, L. Bedrica, J. Pavelić, I. Dikić, M. Katić, M. Kralj, M. H. Bosnar, S. Kapitanović, M. Poljak-Blazi, S. Krizanac, R. Stojković, M. Jurin, B. Subotić, M. Colić, Natural zeolite clinoptilolite: new adjuvant in anticancer therapy, J. Mol. Med. 78 (12) (2001) 708–720, https://doi.org/10.1007/s0010900001765.
[5] K. Pavelic, M. Katic, V. Sverko, T. Marotti, B. Bosnjak, T. Balog, R. Stojkovic, M. Radacic, M. Colic, M. Poljak-Blazi, Immunostimulatory effect of natural clinoptilolite as a possible mechanism of its antimetastatic ability, J. Cancer Res. Clin. Oncol. 128 (1) (2002) 37–44, https://doi.org/10.1007/s00432-001-0301-6.
[6] N. Zarkovic, K. Zarkovic, M. Kralj, S. Borovic, S. Sabolovic, M.P. Blazi, A. Cipak, K. Pavelic, Anticancer and antioxidative effects of micronized zeolite clinoptilolite, Anticancer Res. 23 (2B) (2003) 1589–1595.
[7] M. Katic, B. Bosnjak, K. Gall-Troselj, I. Dikic, K. Pavelic, A clinoptilolite effect on cell media and the consequent effects on tumor cells in vitro, Front. Biosci. 11 (2006) 1722–3172, https://doi.org/10.2741/1918.
[8] L.M. Jurkić, I. Cepanec, S. Kraljevic Pavelić, K. Pavelić, Biological and therapeutic effects of ortho-silicic acid and some ortho-silicic acid-releasing compounds: new perspectives for therapy, Nutr. Metab. 8 (1) (2013) 2, https://doi.org/10.1186/1743-7075-10-2, 10.
[9] K. Pavelić, S. Kraljević Pavelić, Zeolites in medicine, in: Current Achievements and Research of Zeolites in Medicine, Nova Science Publishers, New York, 2019.
[10] S. Kraljević Pavelić, V. Micek, D. Bobinac, E. Bazdulj, A. Gianoncelli, D. Krpan, M. Žuvić, S. Eisenwagen, P.J. Stambrook, K. Pavelić, Treatment of osteoporosis with a modified zeolite shows beneficial effects in an osteoporotic rat model and a human clinical trial, Exp bio med 246 (5) (2020) 529–537.
[11] S. Kraljević Pavelić, D. Krpan, M. Žuvić, S. Eisenwagen, K. Pavelić, Clinical parameters in osteoporosis patients supplemented with PMA-zeolite at the end of 5-year double-blinded clinical trial, Front. Med. 9 (2022), 870962, https://doi.org/10.3389/fmed.2022.870962.
[12] M. Beltcheva, R. Metcheva, N. Popov, S.E. Teodorova, J.A. Heredia-Rojas, A. O. Rodríguez-de la Fuente, L.E. Rodríguez-Flores, M. Topashka-Ancheva, Modified natural clinoptilolite detoxifies small mammal's organism loaded with lead I. Lead disposition and kinetic model for lead bioaccumulation, Biol. Trace Elem. Res. 147 (1–3) (2012) 180–188, https://doi.org/10.1007/s12011-011-9278-4.
[13] A. Mastinu, A. Kumar, G. Maccarinelli, S.A. Bonini, M. Premoli, F. Aria, A. Gianoncelli, M. Memo, Zeolite clinoptilolite: therapeutic virtues of an ancient mineral, Molecules 24 (8) (2019) 1517, https://doi.org/10.3390/molecules24081517.
[14] S. Kraljević Pavelić, L. Saftić Martinović, J. Simović Medica, M. Žuvić, Ž. Perdija, D. Krpan, S. Eisenwagen, T. Orct, K. Pavelić, Clinical evaluation of a defined zeolite-clinoptilolite supplementation effect on the selected blood parameters of patients, Front. Med. 9 (2022), 851782, https://doi.org/10.3389/fmed.2022.851782.
[15] M. Lamprecht, S. Bogner, K. Steinbauer, B. Schuetz, J.F. Greilberger, B. Leber, B. Wagner, E. Zinser, T. Petek, S. Wallner-Liebmann, T. Oberwinkler, N. Bachl, G. Schippinger, Effects of zeolite supplementation on parameters of intestinal barrier integrity, inflammation, redoxbiology and performance in aerobically trained subjects, J Int Soc Sports Nutr 12 (2015) 40, https://doi.org/10.1186/s12970-015-0101-z.
[16] J. Deinsberger, E. Marquart, S. Nizet, C. Meisslitzer, C. Tschegg, K. Uspenska, G. Gouya, J. Niederdöckl, M. Freissmuth, M. Wolzt, B. Weber, Topically administered purified clinoptilolite-tuff for the treatment of cutaneous wounds: a prospective, randomised phase I clinical trial, Wound Repair Regen. 30 (2) (2022) 198–209, https://doi.org/10.1111/wrr.12991.
[17] J. Hao, S. Lang, F. Mante, K. Pavelić, F. Ozer, Antimicrobial and mechanical effects of zeolite use in dental materials: a systematic review, Acta Stomatol. Croat. 55 (1) (2021) 76–89, https://doi.org/10.15644/asc55/1/9.
[18] J. Hao, I. Stavljenić Milašin, Z. Batu Eken, M. Mravak-Stipetic, K. Pavelić, F. Ozer, Effects of zeolite as a drug delivery system on cancer therapy: a systematic review, Molecules 26 (20) (2021) 6196, https://doi.org/10.3390/molecules26206196.
[19] D. Palubinskaite, A. Kantautas, Influence of tribomechanical milling and activation of primary mixtures on the synthesis of calcium silicate hydrates, Mater. Sci. 24 (21) (2006) 395–403.
[20] A.M. Grancarić, A. Tarbuk, D. McCall, Surface modification of polyester fabric with tribomechanically activated natural zeolite (TMAZ) nanoparticles, Polimeri 28 (4) (2007) 219–224.
[21] M. Loizidou, R.P. Townsend, Exchange of cadmium into the sodium and ammonium forms of the natural zeolites clinoptilolite, mordenite, and ferrierite, J. Chem. Soc. Dalton Trans. 18 (1987) 1911–1996.
[22] S. Kraljević Pavelić, V. Micek, A. Filošević, D. Gumbarević, P. Žurga, A. Bulog, T. Orct, Y. Yamamoto, T. Preočanin, J. Plavec, R. Peter, M. Petravić, D. Vikić-Topić, K. Pavelić, Novel, oxygenated clinoptilolite material efficiently removes aluminium from aluminium chloride-intoxicated rats in vivo, Microporous Mesoporous Mater. 249 (2017) 146–156, https://doi.org/10.1016/j.micromeso.2017.04.062.
[23] L.C. Wang, T.T. Zhang, C. Wen, Z.Y. Jiang, T. Wang, Y.M. Zhou, Protective effects of zinc-bearing clinoptilolite on broilers challenged with Salmonella pullorum, Poultry Sci. 91 (8) (2012) 1838–1845, https://doi.org/10.3382/ps.2012-02284.
[24] I. Fornefett, D. Rabet, C. Buttersack, K. Buchholz, Adsorption of sucrose on zeolites, Green Chem. 18 (2016) 3378–3388, https://doi.org/10.1039/C5GC02832A.
[25] S. Berensmeier, K. Buchholz, Separation of isomaltose from high sugar concentrated enzyme reaction mixture by dealuminated β-zeolite, Sep. Purif. Technol. 38 (2004) 129–138.
[26] B. Concepción-Rosabal, G. Rodriguez-Fuentes, R. Simón-Carballo, Development and featuring of the zeolitic active principle fz: a glucose adsorbent, Zeolites 19 (1997) 47–50, https://doi.org/10.1016/S0144-2449(97)00022-5.
[27] B. Hossein Nia, S. Khorram, H. Rezazadeh, A. Safaiyan, A. Tarighat-Esfanjani, The effects of natural clinoptilolite and nano-sized clinoptilolite supplementation on glucose levels and oxidative stress in rats with type 1 diabetes, Can. J. Diabetes 42 (1) (2018) 31–35, https://doi.org/10.1016/j.jcjd.2017.01.010.
[28] D. Hendrichs, Water Treatment Unit Processes Physical and Chemical, CRC Press, Taylor & Francis Group, New York, 2006.
[29] M.K. Doula, Simultaneous removal of Cu, Mn and Zn from drinking water with the use of clinoptilolite and its Fe-modified form, Water Res. 43 (15) (2009) 3659–3672, https://doi.org/10.1016/j.watres.2009.05.037.
[30] R.C. Deka, Acidity in zeolites and their characterization by different spectroscopic methods, Indian J. Chem. Technol. 5 (1998) 109–203.
[31] P.W. Atkins, Physical chemistry, in: Oxford Etc, fifth ed., Oxford University Press, 2009.
[32] Bradfield P. Potter's, Edexcel IGCSE Biology: Student Book, Pearson Education, 2009, 9780435966881.
[33] S.L. Aronoff, K. Berkowitz, B. Shreiner, L. Want, Glucose metabolism and regulation: beyond insulin and glucagon, Diabetes Spectr. 17 (3) (2004) 183–190, https://doi.org/10.2337/diaspect.17.3.183.
[34] M. Al-Shamsi, A. Amin, E. Adeghate, Vitamin E decreases the hyperglucagonemia of diabetic rats, Ann. N. Y. Acad. Sci. 1084 (2006) 432–441, https://doi.org/10.1196/annals.1372.032.
[35] M. Servatan, P. Zarrintaj, G. Mahmodi, S.J. Kim, M.R. Ganjali, M.R. Saeb, M. Mozafari, Zeolites in drug delivery: progress, challenges and opportunities, Drug Discov. Today 25 (4) (2020) 642–656, https://doi.org/10.1016/j.drudis.2020.02.005.
[36] N. Kizilaslan, N.Z. Erdem, The effect of different amounts of cinnamon consumption on blood glucose in healthy adult individuals, Int J Food Sci 2019 (2019), 4138534, https://doi.org/10.1155/2019/4138534.
[37] K. Kubo, Y. Kawai, Zeolite improves high-fat diet-induced hyperglycemia, hyperlipidemia and obesity in mice, J. Nutr. Sci. Vitaminol. 67 (5) (2021) 283–291.
[38] K. Pavelić, M. Hadžija, Medical application of zeolites, in: S.M. Auerbach, K. A. Carrado, P.K. Dutta (Eds.), The Handbook of Zeolite, Science and Technology, Marcel Dekker, New York), 2003, pp. PP1141–1172.
[39] U. Oschilewski, U. Kiesel, H. Kolb, Administration of Silica Prevents Diabetes in BB-Rats, Diabetes., 1985.
[40] B. Kazybay, Q. Sun, K. Dukenbayev, A.A. Nurkesh, N. Xu, A. Kutzhanova, M. Razbekova, A. Kabylda, Q. Yang, Q. Wang, C. Ma, Y. Xie, Network pharmacology with experimental investigation of the mechanisms of rhizoma polygonati against prostate cancer with additional herbzymatic activity, ACS Omega 18 (17) (2022) 14465–14477, https://doi.org/10.1021/acsomega.1c03018, 7.
[41] D.R. Nelson, A.A. Hrout, A.S. Alzahmi, A. Chaiboonchoe, A. Amin, K. Salehi-Ashtiani, Molecular mechanisms behind safranal's toxicity to HepG2 cells from dual omics, Antioxidants 11 (6) (2022) 1125, https://doi.org/10.3390/antiox11061125, 7.
[42] Y. Abdalla, A. Abdalla, A.A. Hamza, A. Amin, Safranal prevents liver cancer through inhibiting oxidative stress and alleviating inflammation, Front. Pharmacol. 1 (12) (2022), 777500, https://doi.org/10.3389/fphar.2021.777500.

[43] S. Abdu, N. Juaid, A. Amin, M. Moulay, N. Miled, Therapeutic effects of crocin alone or in combination with sorafenib against hepatocellular carcinoma: in vivo & in vitro insights, Antioxidants 11 (9) (2022) 1645, https://doi.org/10.3390/antiox11091645, 25.

[44] N. Juaid, A. Amin, A. Abdalla, K. Reese, Z. Alamri, M. Moulay, S. Abdu, N. Miled, Anti-hepatocellular carcinoma biomolecules: molecular targets insights, Int. J. Mol. Sci. 22 (19) (2021), 10774, https://doi.org/10.3390/ijms221910774, 6.

[45] B. Al-Dabbagh, I. A Elhaty, C. Murali, A. Al Madhoon, A. Amin, Salvadora persica (miswak): antioxidant and promising antiangiogenic insights, Am. J. Plant Sci. 9 (2018) 1228–1244, https://doi.org/10.4236/ajps.2018.96091.

[46] W. Wang, Q. Yao, F. Teng, J. Cui, J. Dong, Y. Wei, Active ingredients from Chinese medicine plants as therapeutic strategies for asthma: overview and challenges, Biomed. Pharmacother. 137 (2021), 111383, https://doi.org/10.1016/j.biopha.2021.111383.